doi:10.1246/cl.2011.1376

Published on the web November 26, 2011

Urea-induced Direct Synthesis of Nanostructured α-$Ni(OH)_2$ on Nickel Foam

Sa Lv[1,2] and Shuangxi Xing*[1]
[1]*Institute of Colloid and Interface Chemistry, Faculty of Chemistry, Northeast Normal University, Changchun 130024, P. R. China*
[2]*Jilin Institute of Architecture and Civil Engineering, Changchun 130118, P. R. China*

(Received August 11, 2011; CL-110673; E-mail: xingsx737@nenu.edu.cn)

A convenient hydrothermal route was designed for the direct synthesis of nanostructured α-$Ni(OH)_2$ on nickel foam in an aqueous solution only containing $Ni(NO_3)_2$ and urea. The obtained urchin-like $Ni(OH)_2$ displayed good electrochemical activity with a maximum specific capacitance of $103\,mA\,h\,g^{-1}$ at a current density of $2.5\,A\,g^{-1}$.

In recent years, $Ni(OH)_2$ has attracted extraordinary interest owing to unique size- and shape-dependent properties and widespread applications in catalysts, batteries, gas sensors, fuel-cell electrodes, etc.[1,2] In particular, $Ni(OH)_2$ as a promising active electrode material possesses several significant advantages, including low cost, low toxicity, and high pseudocapacitive behavior in Ni-based alkaline batteries.[3,4] $Ni(OH)_2$ has a hexagonal layered structure with two polymorphs, α- and β-phases.[5] Normally, α-$Ni(OH)_2$ exhibits superior electrochemical properties compared with the β-$Ni(OH)_2$.[6,7] Apart from the crystal structure, the morphology of $Ni(OH)_2$ has significant influence on its electrochemical properties.[4,8] Therefore, much effort has been focused on modifying synthetic strategies that could provide the desired control for the morphology of the $Ni(OH)_2$ nanostructures and optimize their properties thereby.[5,9–11]

For electrochemical applications, the resulting nanostructures are generally acquired by mixing them with a binder and carbon black and then pressing onto substrates to fabricate electrodes. This process inevitably introduces additional undesirable interfaces in the electrode material.[12] To solve this question and avoid a complex process, some of the above approaches have been extended to grow active electrode material directly on solid substrates, which were realized by electrodeposition, chemical bath deposition, or plasma-assisted oxidation.[13–15] Nanostructured $Ni(OH)_2$ and NiO electrodes have been achieved in this way. Such a direct growth manner benefits forming strong adherence between materials and the substrate surface. Especially, with no complex assembly, it facilitates the electrochemical measurements and manipulation process.

Here, we describe a facile urea-induced hydrothermal method for direct synthesis of nanostructured α-$Ni(OH)_2$ on nickel foam in a system only containing $Ni(NO_3)_2$, urea, and water. This approach allows for an easy manipulation process to make electrodes. Furthermore, the electrochemical performance of the as-obtained $Ni(OH)_2$ electrode was investigated.

In a typical procedure, an aqueous solution (36 mL) containing $Ni(NO_3)_2 \cdot 6H_2O$ (9 mmol), urea (3 mmol), and precleaned nickel foam was sealed into a 50-mL Teflon-lined autoclave and heated at 120 °C for 24 h.

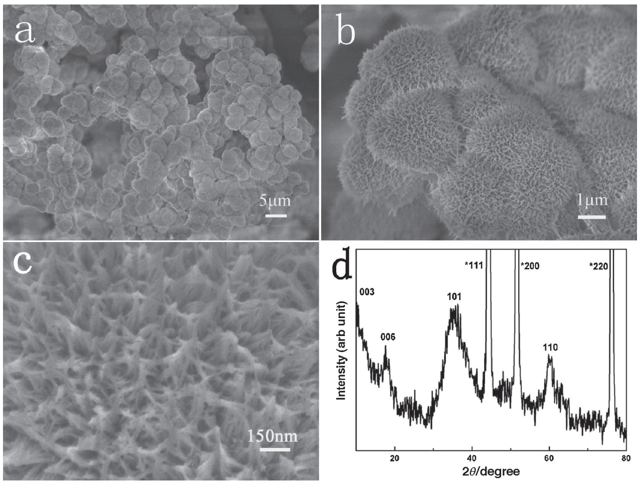

Figure 1. (a–c) FE-SEM images of $Ni(OH)_2$ nanostructures at different magnifications, (d) XRD pattern of the samples.

Figure 1 shows SEM images of the products at different magnifications. After reaction, $Ni(OH)_2$ spheres with a mean diameter of ca. 3 μm are obtained, and they are packed closely with each other (Figure 1a). The spheres give urchin-like surface structure, and they are composed of entangled network nanofibers in high density (Figure 1b). These nanofibers grow radially with average diameter of less than 20 nm, and they emerge as clusters that are crosslinked with each other (Figure 1c). A corresponding XRD pattern is provided in Figure 1d, and all diffraction peaks are in good agreement with the pattern of α-$Ni(OH)_2$ (JCPDS card no. 22-0444) in addition to the peaks marked with asterisks that are attributed to the nickel foam substrate (JCPDS 03-1051).[3,16]

In order to understand the growth mechanism of the $Ni(OH)_2$ nanostructures, a control experiment was performed, where NaOH was utilized as alkali sources instead of urea under otherwise the same conditions. In this system, plate-like $Ni(OH)_2$ was obtained. Several plates are agglomerated together, and each plate is composed of a stack of highly close-packed nanoflakes with a thickness of about 20 nm (Figure S1 in Supporting Information; SI).[19]

The formation of distinct morphologies by changing precipitants should originate from their different reaction processes. When urea was exploited as precipitant, NH_3 and CO_2 were produced from the decomposition of urea around 70 °C, and the following hydrolysis resulted in the presence of OH^- and CO_3^{2-} in the solution. Therefore, urea provided a steady OH^- ion supply via hydrolysis, and OH^- ion was slowly released.[5] Under this condition, the reaction between the nickel ions and OH^- ions was readily controllable, and a relatively slow nucleation rate was thus achieved. Finally, a thermo-

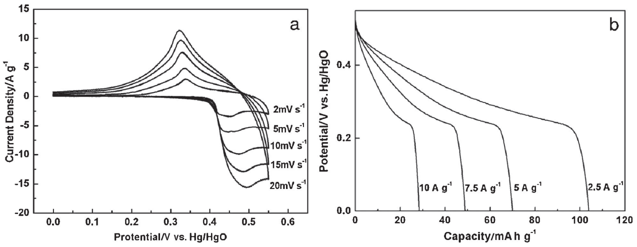

Figure 2. Electrohemical properties of $Ni(OH)_2$ in 2 M KOH solution: (a) CV curves at different scan rates; (b) discharge curves at different discharge current densities.

dynamically controled process led to the generation of urchin-like α-$Ni(OH)_2$ spheres.[9,17] On the contrary, when NaOH was directly added to the $Ni(NO_3)_2$ solutions, precipitation occurred immediately. The rapid nucleation and growth process caused the formation of highly close-packed nanoflakes.

CV and constant current discharge measurements have been used to evaluate the electrochemical properties and quantify the specific capacitance of the as-prepared $Ni(OH)_2$ electrode. Figure 2a shows the CV curves of the $Ni(OH)_2$ electrode at different scan rates ranging from 2 to 20 $mV\,s^{-1}$. The shape of the CV curves indicates that the capacitance is distinct from that of electric double-layer capacitance, where the shape is normally close to an ideal rectangular shape.[15,18] In this case, a couple of redox peaks are visible in the potential range of 0–0.55 V. Such peaks are related to Faradaic reaction of $Ni(OH)_2$ corresponding to the following well-accepted reaction:[6]

$$Ni(OH)_2 + OH^- \rightleftarrows NiOOH + H_2O + e^- \qquad (1)$$

This suggests that the measured capacity mainly originates from the pseudo-capacitance that arises from a reversible redox mechanism. It should be noted that the current density increases with scan rate, and the shape of the CV curves changes accordingly (Figure 2). The anodic and cathodic peak potentials shift to more positive and negative positions, respectively, and the capacitance decreased inevitably. Moreover, a control experiment by using pristine nickel foam as electrode was carried out, and no well-defined peaks could be observed in the CV curve compared to the presence of two strong redox peaks visible at $Ni(OH)_2$ on nickel foam (Figure S2 in SI).[19] This confirms the electrochemical performance mainly originates from the nanostructured $Ni(OH)_2$ other than the nickel foam.

The typical constant current discharge test on the $Ni(OH)_2$ electrode in the potential range of 0–0.5 V was further carried out at various current densities (Figure 2b). The specific capacitance decreases from 103 to 29 $mA\,h\,g^{-1}$ as the discharge current density increases from 2.5 to 10 $A\,g^{-1}$. As the discharge current density increases, a large voltage drop is produced and finally the specific capacitance decreases (Figure 2b). The decrease in capacitance is probably attributed to the diffusion effect; that is, the inner active sites in the electrode are inaccessible at higher charge–discharge current densities. Therefore, the specific capacitance obtained at the smaller charge–discharge current densities is believed to be closer to that of a state with sufficient utilization of the electrode material.[6,15]

In our synthetic system, the nanostructured $Ni(OH)_2$ directly formed on the nickel foam showed good electrochemical activity. On one hand, the hydrothermal process allowed the direct formation of $Ni(OH)_2$ onto the nickel foam, and a electrical and mechanical adherence was achieved between the electrode materials and the substrate. On the other hand, nickel foam has high electronic conductivity and desirable 3D structure, which reduces the diffusion resistance of electrolytes, and provides a high specific surface area for sufficient loading active $Ni(OH)_2$ material on it and maintains smooth electron pathways.

In summary, by employing a facile hydrothermal strategy, nanostructured α-$Ni(OH)_2$ directly synthesized on nickel foam was achieved by introducing urea as alkali source. The obtained $Ni(OH)_2$ electrode presented a good electrochemical capacity of 103 $mA\,h\,g^{-1}$ at a current density of 2.5 $A\,g^{-1}$. The good electrochemical performance could be ascribed to the effective utilization of the active materials and this made the α-$Ni(OH)_2$ a promising material for supercapacitors or rechargeable batteries.

This work was supported by National Natural Science Foundation of China (Grant No. 21103018) and Jilin Provincial Science and Technology Development Foundation (Grant No. 201101010).

References and Notes

1 H. Cao, H. Zheng, K. Liu, J. H. Warner, *ChemPhysChem* **2010**, *11*, 489.
2 G. Duan, W. Cai, Y. Luo, F. Sun, *Adv. Funct. Mater.* **2007**, *17*, 644.
3 Y. Luo, G. Li, G. Duan, L. Zhang, *Nanotechnology* **2006**, *17*, 4278.
4 F. Tao, M. Guan, Y. Zhou, L. Zhang, Z. Xu, J. Chen, *Cryst. Growth Des.* **2008**, *8*, 2157.
5 L. Xu, Y.-S. Ding, C.-H. Chen, L. Zhao, C. Rimkus, R. Joesten, S. L. Suib, *Chem. Mater.* **2008**, *20*, 308.
6 G. Hu, C. Li, H. Gong, *J. Power Sources* **2010**, *195*, 6977.
7 H. B. Liu, L. Xiang, Y. Jin, *Cryst. Growth Des.* **2006**, *6*, 283.
8 D. Yang, R. Wang, M. He, J. Zhang, Z. Liu, *J. Phys. Chem. B* **2005**, *109*, 7654.
9 L. Dong, Y. Chu, W. Sun, *Chem.—Eur. J.* **2008**, *14*, 5064.
10 X. Ni, Q. Zhao, J. Cheng, H. Zheng, B. Li, D. Zhang, *Chem. Lett.* **2005**, *34*, 1408.
11 C. Tang, G. Li, L. Li, *Chem. Lett.* **2008**, *37*, 1138.
12 J. Liu, Y. Li, X. Huang, R. Ding, Y. Hu, J. Jiang, L. Liao, *J. Mater. Chem.* **2009**, *19*, 1859.
13 B. Varghese, M. V. Reddy, Z. Yanwu, C. S. Lit, T. C. Hoong, G. V. S. Rao, B. V. R. Chowdari, A. T. S. Wee, C. T. Lim, C.-H. Sow, *Chem. Mater.* **2008**, *20*, 3360.
14 G.-W. Yang, C.-L. Xu, H.-L. Li, *Chem. Commun.* **2008**, 6537.
15 U. M. Patil, K. V. Gurav, V. J. Fulari, C. D. Lokhande, O. S. Joo, *J. Power Sources* **2009**, *188*, 338.
16 X. Song, L. Gao, *J. Phys. Chem. C* **2008**, *112*, 15299.
17 L.-X. Yang, Y.-J. Zhu, H. Tong, Z.-H. Liang, W.-W. Wang, *Cryst. Growth Des.* **2007**, *7*, 2716.
18 J.-W. Lang, L.-B. Kong, W.-J. Wu, Y.-C. Luo, L. Kang, *Chem. Commun.* **2008**, 4213.
19 Supporting Information is available electronically on the CSJ-Journal Web site, http://www.csj.jp/journals/chem-lett/index.html.